minerals

MDPI

Article

Predictive Model of Setting Times and Compressive Strengths for Low-Alkali, Ambient-Cured, Fly Ash/Slag-Based Geopolymers

Supphatuch Ukritnukun [1], Pramod Koshy [1,*], Aditya Rawal [2], Arnaud Castel [3,4] and Charles Christopher Sorrell [1]

[1] School of Materials Science and Engineering, UNSW Sydney, Sydney 2052, Australia; usupphatuch@gmail.com (S.U.); C.Sorrell@unsw.edu.au (C.C.S.)
[2] NMR Facility, Mark Wainwright Analytical Centre, UNSW Sydney, Sydney 2052, Australia; a.rawal@unsw.edu.au
[3] School of Civil and Environmental Engineering, UNSW Sydney, Sydney 2052, Australia; Arnaud.Castel@uts.edu.au
[4] School of Civil and Environmental Engineering, University of Technology, Sydney 2007, Australia
* Correspondence: koshy@unsw.edu.au

Received: 16 August 2020; Accepted: 5 October 2020; Published: 17 October 2020

Abstract: The effects of curing temperature, blast furnace slag content, and Ms on the initial and final setting times, and compressive strengths of geopolymer paste and mortars are examined. The present work demonstrates that ambient-cured geopolymer pastes and mortars can be fabricated without requiring high alkalinity activators or thermal curing, provided that the ratios of Class F fly ash (40–90 wt%), blast furnace slag (10–60 wt%), and low alkalinity sodium silicate (Ms = 1.5, 1.7, 2.0) are appropriately balanced. Eighteen mix designs were assessed against the criteria for setting time and compressive strength according to ASTM C150 and AS 3972. Using these data, flexible and reproducible mix designs in terms of the fly ash/slag ratio and Ms were mapped and categorised. The optimal mix designs are 30–40 wt% slag with silicate modulus (Ms) = 1.5–1.7. These data were used to generate predictive models for initial and final setting times and for ultimate curing times and ultimate compressive strengths. These projected data indicate that compressive strengths >100 MPa can be achieved after ambient curing for >56 days of mixes of ≥40 wt% slag.

Keywords: geopolymers; ambient curing; low alkalinity; setting time; compressive strength

1. Introduction

Ordinary Portland cement (OPC) is an indispensable structural material for civil and construction applications. However, high levels of CO_2 are released during the production cycle of OPC (0.65–1.0 ton of CO_2 per ton of OPC) [1,2]. Currently, global cement production contributes 5–8% of the annual anthropogenic global CO_2 emissions [2,3], with this issue expected to worsen with increased cement consumption in the coming decades.

Numerous formulations have been investigated as low-CO_2 alternatives to OPC. The first generation was blended cements, in which supplementary cementitious materials (SCMs), viz., metakaolin, fly ash, ground granulated blast furnace slag (GGBFS), or silica fume, were added to OPC [3]. The second generation includes geopolymer cements and concretes, which do not contain OPC [4,5]. Geopolymers must meet the mechanical strength, setting time, and workability and durability requirements of construction materials.

OPC- and blended cement-based mortars require only water addition to initiate the hydration reactions for hardening and strength development [6]. On the other hand, geopolymer-based mortars and concretes involve a completely different chemical mechanism for hardening and strength development. The raw materials for geopolymers include SCMs (aluminosilicates to provide the necessary Si and Al for the geopolymer), alkaline activators (alkali metal silicates or hydroxides for dissolving the raw materials, to provide hydroxyl groups, and to establish charge balance), and water (to improve workability and act as a solvent for the activators).

The geopolymer network is comprised of tetrahedral silicate and aluminate structural units in a three-dimensional network linked by Si-O-Si and Si-O-Al covalent bonds (with terminal oxygens saturated to form hydroxyl groups) [7]. While SiO_4 tetrahedra are charge balanced, the AlO_4 tetrahedra require charge balance from alkali ions (Na^+ or K^+). The geopolymer mortars are subjected to ambient or elevated thermal curing (40–80 °C) for hardening and strength development [8,9]. The mechanical properties are dominated by the resultant microstructures, which may degrade the compressive strength through the presence of residual undissolved SCMs [10], excess alkaline activators [11], and a closed or open pore network (porosities of 5–10%) [12–15].

The application of geopolymers as a replacement for OPC involves several comparative technical and performance considerations:

- Geopolymers and OPC are cementitious materials that are gelled in alkaline environments, with geopolymers generally requiring higher pH and elevated curing temperatures than for OPC [6,7];
- Reduction in CO_2 emissions (in the range ~9–64% relative to OPC production, depending on the choice of raw materials, mix design, curing regime, and the location of the batching plant, which involves the transportation of raw materials) [1,16–19];
- Reduction in energy consumption through the elimination of cement clinker production (savings of ~3.7 GJ per ton of cement production) [20];
- Increase in fire resistance from 300–400 °C for OPC to 800–1000 °C for geopolymers [7,21];
- Potential increase in compressive strength from 40–50 MPa for OPC standard mortars to 50–80 MPa for geopolymer mortars [8,9,22];
- Greater utilisation of industrial by-products, which then are diverted from landfill [6,7];
- Greater compliance with emerging environmental regulations concerning production and disposal of waste and reduction in greenhouse gas emissions [7].

Class C fly ash is used rarely, owing to its relatively high pH (>10), which causes flash setting [23]. In contrast, Class F fly ash has been investigated frequently as a geopolymer raw material [7,24,25] owing to its low pH (<8) [23]. Low-calcium fly ash is comprised largely of the reactive components, amorphous SiO_2 and Al_2O_3, which are the principal network-forming cations in the geopolymerisation process [26]. In effect, systems using alkali activators with Class F fly ash (sodium aluminate silicate hydrate (N-A-S-H) or potassium aluminate silicate hydrate (K-A-S-H)) exhibit low compressive strengths when air-tight cured, although thermal curing [8,9,27,28] and use of high concentrations of alkaline activators (4.5–16.5 M NaOH and/or sodium silicate Ms = 0.96–1.40) [13,29–31] are required.

Thermally cured, Class F fly ash-based, geopolymer concretes have exhibited excellent mechanical strengths and durabilities in different tests [32–38]. If slag is the sole aluminosilicate source, an Al-Si tetrahedral geopolymer structure is not formed, owing to its low Al content. This deficiency is overcome by adding blast furnace slag to the fly ash, which increases the proportion of AlO_4 tetrahedra [39,40]. The enhanced strengths and durabilities have resulted in these becoming the most commonly investigated geopolymer systems (N-C-A-S-H and K-C-A-S-H). When NaOH is the activator, then the Ca hydrates and subsequently combines with the Si in solution to form calcium silicate hydrate (C-S-H) [39,41]. When sodium silicate is the activator, both the Si and Al form tetrahedra in a calcium aluminate silicate hydrate (C-A-S-H) geopolymer network. These silicate solutions are defined in terms of the silicate modulus Ms, which is the SiO_2/M_2O molar ratio (where M is an alkali metal) [42]. Since there is a direct correlation between the high proportion of AlO_4 tetrahedra

and compressive strength [43], but a reverse correlation between the compressive strength and the Ms [44,45], then it is clear that lower values of Ms result in higher proportions of AlO_4 tetrahedra and hence, geopolymerisation.

The increased applicability of Class F fly ash geopolymers has been hindered by low compressive strengths following ambient curing, the consequent necessity of accelerating the kinetics by thermal curing, and the use of high-alkalinity activators (4.5–16.5 M NaOH and/or sodium silicate Ms = 0.96–1.40). These issues impact on the potential to fabricate on-site and pose risks to personal safety and they have been addressed by five main strategies:

1. *Curing Conditions*: Curing in air-tight conditions can improve the strengths [46].
2. *Accelerated Kinetics by Mechanical Activation*: The reactivity can be increased by comminution of the fly ash [13,22,47].
3. *Cementitious Material Compositions*: On-site fabrication can be made feasible by accelerating the setting rate by increasing the calcium content by adding slag and high-calcium fly ash or $Ca(OH)_2$ as an activator [14,25,44,48,49].
4. *Alkali Hydroxide Molarity*: The issue of NaOH corrosiveness has been addressed by reducing the molarity of the NaOH solution [29,50].
5. *Sodium Silicate/Alkali Hydroxide Ratio:* The corrosiveness of NaOH also has been addressed by increasing the proportion of sodium silicate relative to NaOH [40,51].

Table 1 provides comprehensive summaries of the published data reporting the outcomes of applying the preceding five strategies in terms of the compositions, curing conditions, and compressive strengths of ambient-cured geopolymer mortars. More details are provided in the following text.

Therefore, the aim of the present work is to investigate potential solutions to address the issues of on-site fabrication and personal safety by investigating ambient temperature curing, chemical activation by varying the fly ash/slag mass ratio (FA/S), and varying the Ms. The properties of the geopolymer pastes and mortar systems were assessed against the criteria for setting time and compressive strength according to ASTM C150 for Type 1 cement and Australian Standard AS 3972 for General Purpose (GP) cement, as shown in Table 2.

2. Materials and Methods

2.1. Materials

2.1.1. SCMs

The aluminosilicate materials used were a Class F fly ash (Eraring Power Station, Eraring, Australia) and ground granulated blast furnace slag (Blue Circle Southern Cement Limited, Sydney, Australia). The latter is referred to as blast furnace slag or slag for the remainder of the manuscript. Both Class F fly ash and blast furnace slag comply with the requirements stated in AS 3582.1 and AS 3582.2, respectively. The chemical compositions of the samples were determined by wavelength-dispersive X-ray fluorescence (WDXRF; PanAlytical Axios Advanced WDXRF, 4 kW, Almelo, The Netherlands) and are shown in Table 3.

Table 1. Comprehensive summary of geopolymer mortars cured in air-tight conditions at room temperature.

Aluminosilicate Source [1]		Alkaline Activator Proportions			Mix [3] A:L:S	w/b [4]	Specimen		Curing Conditions		Compressive Strength (MPa)	Reference
		Components		Mix								
Fly Ash	Slag	Na_2SiO_3	NaOH	Silicate Modulus [2]			Shape	Size (mm)	Temperature (°C)	Age (Day)		
70%	30%	Ms = 2.78	14 M	Ms = 1.20	1.0:0.4:1.6	0.20	Cube	50 × 50 × 50	23	28	65.0	[40]
80%	20%										48.0	
90%	10%										40.0	
100%	-										26.0	
-	100%	Ms = 2.06	15 M	Ms = 0.96	1.0:0.75:2.75	0.66	Cube	50 × 50 × 50	20	28	39.6	[52]
10%	90%										48.2	
20%	80%										53.3	
30%	70%										47.3	
40%	60%										55.6	
50%	50%										62.5	
100%	-	Ms = 2.39	6 M	Ms = 1.52	1.0:0.6:1.0	-	Cube	50 × 50 × 50	25	28	38.5	[45]
			10 M	Ms = 1.25							50.5	
			14 M	Ms = 1.06							56.0	
-	100%	Ms = 2.03	-	Ms = 1.00	1.0:0.16:2.75	0.35	Cube	50 × 50 × 50	25	28	73.0	[53]
50%	50%										98.0	
100%	-										22.0	
-	100%					0.50					64.0	
50%	50%										89.0	
100%	-										20.0	
-	100%					0.65					35.0	
50%	50%										30.0	
100%	-										19.0	
40%	60%	Ms = 3.41	-	Ms = 1.40	1.0:0.57:3.0	0.45	Cube	40 × 40 × 40	20	28	59.0	[54]
50%	50%										52.0	
60%	40%										43.0	

[1] Percentages are wt%; [2] Final silicate modulus (Ms) was calculated from mass ratio given in the study; [3] A:L:S = Aluminosilicate (fly ash + slag): Liquid alkaline activator (Na_2SiO_3 + NaOH): Sand ratio by mass; [4] w/b = water / binder ratio by mass.

Table 2. Performance requirements for General Portland (GP) cement according to ASTM C150 and AS 3972 [55,56].

Parameter	Criteria	ASTM C150 Type I	AS 3972 Type GP
Setting Time	Minimum	45 min	45 min
	Maximum	375 min	360 min
Mortar Compressive Strength	3 days (min)	12 MPa	-
	7 days (min)	19 MPa	35 MPa
	28 days (min)	-	45 MPa

Table 3. Chemical compositions of raw materials by X-ray fluorescence.

Oxide	Fly Ash (wt%)	Slag (wt%)
SiO_2	64.63	33.84
Al_2O_3	24.40	13.76
Na_2O	0.73	0.38
K_2O	2.31	0.28
CaO	1.68	41.75
MgO	0.63	5.59
Fe_2O_3	2.91	0.56
SO_3	0.14	2.42
Loss on Ignition (LOI)	1.34	0.13
Total	98.77	98.71

A Philips X'pert MPD (Multi-Purpose X-ray Diffraction System, 40 mA, 45 kV, CuKα radiation, 10–70° 2-theta range, 0.026° 2-theta min^{-1} speed; Amsterdam, The Netherlands) was used to determine the phases present in the samples (Figure 1). The main crystalline components in the fly ash were quartz (SiO_2), mullite ($3Al_2O_3{\cdot}2SiO_2$), and hematite (Fe_2O_3). A broad amorphous hump between 18° and 30° 2θ is attributed to aluminosilicate glass [25]. The pattern for the blast furnace slag is predominantly amorphous, as indicated by the broad hump at 22° and 38° 2θ, which is attributed to calcium aluminosilicate glass [25,57]. There also are small but detectable quantities of calcite ($CaCO_3$) and gypsum ($CaSO_4{\cdot}2H_2O$). The particle size distributions of the samples were determined by laser diffraction using a Malvern Mastersizer 2000 instrument, Worcestershire, UK. The mean particle size of fly ash was 16.4 μm and that of slag was 13.3 μm.

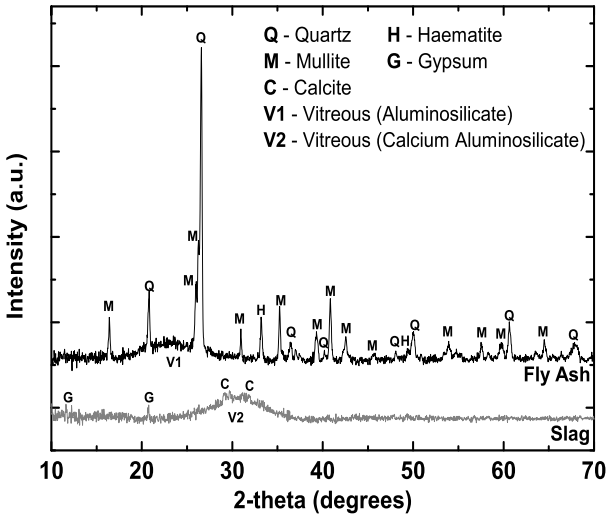

Figure 1. X-diffraction patterns of Class F fly ash and blast furnace slag, where Q—Quartz; M—Mullite; C—Calcite; H—Hematite; G—Gypsum; V1—Vitreous (aluminosilicate); V2—Vitreous (calcium aluminosilicate).

2.1.2. Alkaline Activator

The alkaline activators were mixtures of sodium hydroxide (NaOH) and sodium silicate solution. NaOH pellets (98% purity), Ajax FineChem, Univar A-302, Scoresby, Australia, were added to adjust the molar ratio of the sodium silicate solutions and hand-mixed until dissolution was observed. The alkaline activators (Ms = 1.5, 1.7, and 2.0) then were homogenised for 24 h prior to casting. The sodium silicate solution, Grade D, PQ Australia, Dandenong, Australia, had a chemical composition of SiO_2 = 29.4 wt%, Na_2O = 14.7 wt%, and H_2O = 55.9 wt% with Ms = 2.0. Figure 2 shows the measured pH values of the activator solutions in comparison to OPC.

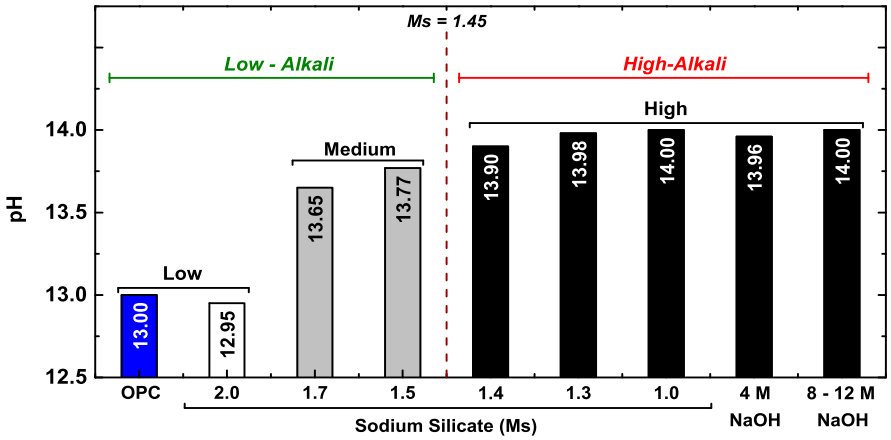

Figure 2. pH values of aqueous solutions of Na_2SiO_3 (Ms = 1.0–2.0) and NaOH (4–12 M) in comparison to Portland cement slurry determined in the present work; proposed classification according to Davidovits [7].

2.1.3. Fine Aggregate

The fine aggregate used in this present work was washed beach sand (BC Sands, Sydney, NSW, Australia), with a true density of 2650 kg·m^{-3} and water absorption of 3.5%, both determined according to ASTM C128-15 [58]. Following rinsing with running tap water on a sieve for 5 min, the sand was oven dried at 105 °C for 48 h and then, prepared to a saturated surface dry (SSD) state prior to batching by adding 3.5 wt% water [6].

2.1.4. Mix Design

The mass of geopolymer binder is the sum of the masses of the SCMs (fly ash and blast furnace slag), NaOH, and the SiO_2 and Na_2O in the sodium silicate. The mass of water is the sum of the masses of that in the sodium silicate solution and that of free water used to standardise the mixes. Since typical water/binder mass ratios in geopolymer mortars range from 0.3 to 0.7 [59], the minimal value of 0.3 was selected, which was sufficient for workability but minimised apparent porosity. Other data for similar mixes [60–62] showed that the compressive strengths were highest in the mass ratio of alkaline activator to geopolymer binder range of 0.5–0.7. The minimal value of 0.5 was selected on the basis of cost considerations. Other data [63] showed minimal strength variation for a sand to geopolymer binder mass ratio of 0.5–1.5, workability difficulty at ratios >1.5, and a significant decrease in the compressive strength in the range 2.0–3.0 [64]. The maximal value of 1.5 was selected based on these considerations. The mix proportions are given in Table 4.

Table 4. Geopolymer mortar mix proportions (kg·m^{-3}).

Mix No. [1]	FA/S [2]	Fly Ash	Slag	Na_2SiO_3	NaOH	Sand [3]	Free Water
Ms = 2.0							
1	90/10	641.4	71.3	356.3	0.0	1069.0	62.0
2	80/20	570.1	142.5	356.3	0.0	1069.0	62.0
3	70/30	498.9	213.8	356.3	0.0	1069.0	62.0
4	60/40	427.6	285.1	356.3	0.0	1069.0	62.0
5	50/50	356.3	356.3	356.3	0.0	1069.0	62.0
6	40/60	285.1	427.6	356.3	0.0	1069.0	62.0
Ms = 1.7							
7	90/10	638.4	70.9	340.9	13.8	1064.0	72.0
8	80/20	567.5	141.9	340.9	13.8	1064.0	72.0
9	70/30	496.5	212.8	340.9	13.8	1064.0	72.0
10	60/40	425.6	283.7	340.9	13.8	1064.0	72.0
11	50/50	354.7	354.7	340.9	13.8	1064.0	72.0
12	40/60	283.7	425.6	340.9	13.8	1064.0	72.0
Ms = 1.5							
13	90/10	636	70.7	330.2	23.1	1060.0	80.0
14	80/20	565.3	141.3	330.2	23.1	1060.0	80.0
15	70/30	494.7	212.0	330.2	23.1	1060.0	80.0
16	60/40	424.0	282.7	330.2	23.1	1060.0	80.0
17	50/50	353.3	353.3	330.2	23.1	1060.0	80.0
18	40/60	282.7	424.0	330.2	23.1	1060.0	80.0

[1] Mix proportions were designed to ensure a final unit weight of 2200 kg·m^{-3}; [2] FA/S = Fly ash/Slag mass ratio; [3] Sand in the saturated surface dry (SSD) condition.

2.1.5. Mixing, Sample Preparation, and Curing

The geopolymer mortars were prepared in the following sequence:

- The fly ash and blast furnace slag were dry mixed in a 5 L Hobart mixer for 3 min.
- The alkaline activator solution was added to the mix and blended in the Hobart mixer for 5 min in order to activate the fly ash and blast furnace slag.
- Sand was added and the mixing continued for a further 5 min.
- The majority of the blended mix was transferred to a brass mould and spread into sixteen individual mould cavities.
- Mould filling was optimised by vibratory casting for 3 min on a vibrating table.
- Insufficient filling was compensated by supplementation from the remainder in the Hobart mixer bowl; excess filling was removed by guillotine scraping. These procedures were followed by additional vibratory casting for 1 min.
- The mould was placed in a zip-lock plastic bag and sealed without removing excess air.
- The cast samples were cured for 24 h at 23 ± 2 °C.
- The samples were removed from the mould, placed in an air-tight plastic container (7 L volume), which contained a bowl of water (200 mL volume), and retained as such until testing.

2.2. Methods

2.2.1. Setting Time

The time of setting of each geopolymer paste was determined using a Vicat needle in accordance with ASTM C191-13 [65]. The needle used was 1.00 ± 0.05 mm in diameter. The time of setting is measured in terms of initial and final setting times.

2.2.2. Compressive Strength

The compressive strengths were measured by uniaxial compressive strength testing according to ASTM C109-13. Geopolymer mortar cubes of 25 × 25 × 25 mm^3 dimensions were used instead of the required 50 × 50 × 50 mm^3 dimensions [66], since the maximal load was only 100 kN. An Instron 5982 universal testing machine (Waltham, MA, USA) was used to apply force at a loading rate of 1200 $N{\cdot}s^{-1}$ to a pair of the vertical cast sides of the prism. Four samples for each composition and time point were tested after 1, 7, 14, and 28 days of ageing.

Owing to the statistical distribution of flaw sizes in brittle materials, smaller samples are expected to yield higher strengths than larger ones [67]. Data of Hamad [68] for compressive strength as a function of cube edge length suggest that these two variables exhibit linear relationships for different time points. Therefore, for comparison of the results with work done by others, the ratios of the compressive strengths were used to generate conversion factors, which are listed in Table 5.

Table 5. Size conversion factor for compressive strength data [68].

Cube Specimen (mm^3)	Compressive Strength (MPa)		Conversion Factor		Nature of Data
	7 Days	28 Days	7 Days	28 Days	
150 × 150 × 150	11.40	15.80	0.70	0.68	Determined
100 × 100 × 100	14.20	19.00	0.87	0.81	Determined
50 × 50 × 50	15.00	21.80	0.92	0.93	Determined
25 × 25 × 25	16.23	23.37	1.00	1.00	Extrapolated

3. Results

3.1. Setting Time

Figure 3 shows the influence of blast furnace slag content for varying Ms on the setting time for ambient-cured geopolymer pastes. The data for those containing only fly ash are not reported owing to the excessive setting times, which revealed failure to set even after one week; this behaviour has been confirmed elsewhere [7,69]. Conversely, the data for the geopolymer pastes containing ≥70 wt% blast furnace slag are not reported because they set within 20 min of mixing and therefore, were not suitable for casting.

Table 2 shows that the initial and final setting times are in a processing window between 45 and 360–375 min, respectively; the boxes in Figure 3 indicate the samples that meet these recommendations. The shift in the boxes shows that the setting times decrease with both increasing blast furnace slag content and Ms. These are in agreement with the results of other studies [39,40,70].

More specifically, Figure 3 shows that the blast furnace slag contents within the processing window for all three Ms are 20–30 wt%. Consequently, this range also is predictive of the slag contents most likely to be applicable for ambient-cured geopolymer pastes of varying Ms. The effect of the Ms on the rate of setting clearly shows the influence of the chemical composition of the alkaline activator. The presence of soluble silica modifies the reaction kinetics and rate of geopolymerisation by enhancing the process of condensation of the dissolved geopolymer precursors, and this has the effect of accelerating the polymerisation process [71].

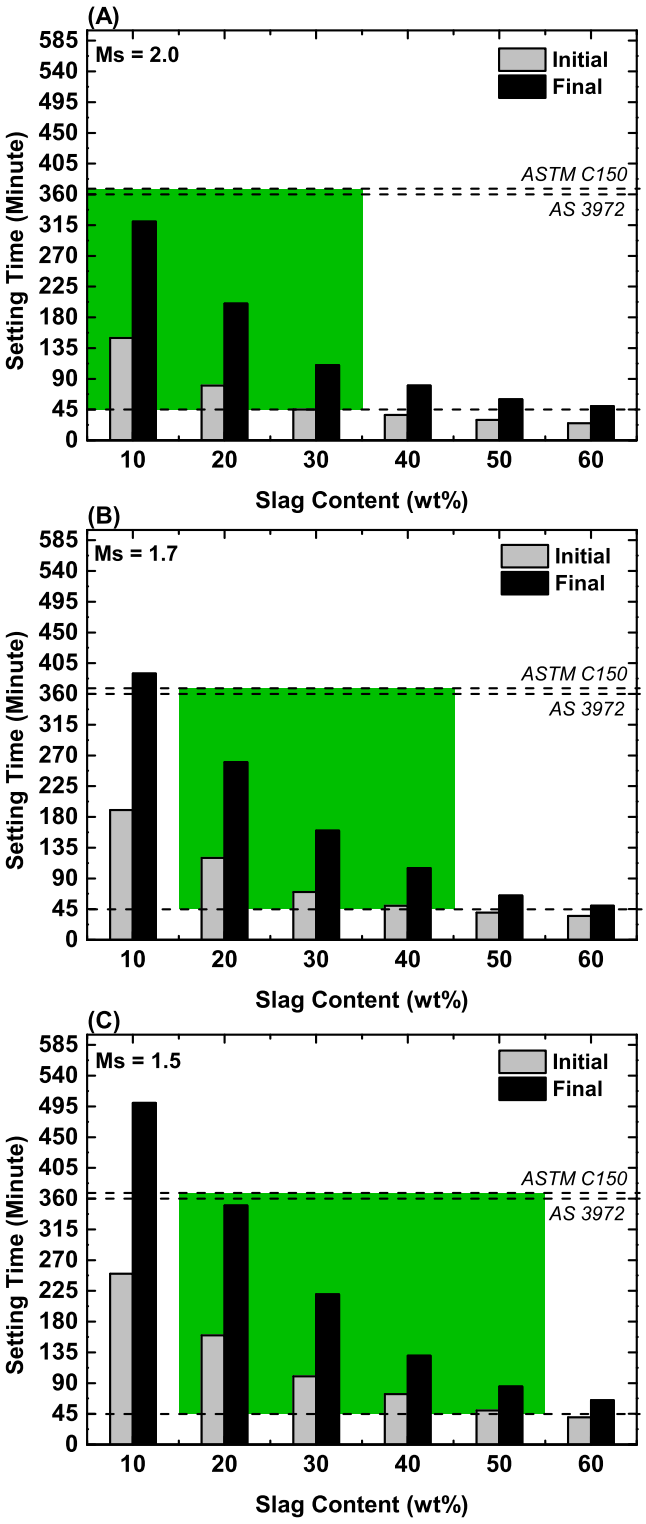

Figure 3. Effect of blast furnace slag content on the setting times of ambient-cured geopolymer pastes for (**A**) Ms = 2.0, (**B**) Ms = 1.7, and (**C**) Ms = 1.5. The dashed lines represent the requirements for the minimal initial setting time (45 min) and maximal final setting time (360–375 min).

For the fly ash/blast furnace slag mixtures that were examined, both the initial and final setting times decreased exponentially with increasing blast furnace slag content. Since the initial setting time is equivalent to the maximal working time and the final setting time is equivalent to the minimal hardening time, these two sets of data have been fit to generic equations in order to allow prediction

of these times as a function of blast furnace slag content and Ms (at an alkaline activator/SCMs mass ratio of 0.5, water/binder mass ratio of 0.3); these data are plotted in Figure 4. The extrapolations to initial and final setting times at low slag content do not intersect the ordinates, since the chemistry and hence, the models for compositions without slag are different from those with slag; the limits of these regions are arbitrary. Although these intersections were not examined in the present work owing to the presumption that excessive setting times would be required, other works [7,40,69] have shown that these intersections would occur at times >24 h (1440 min); the present work has revealed that final setting of this composition did not occur even after 7 days (10,080 min). The fits between the experimental and calculated values for these slag-containing compositions indicate that the setting behaviour of ambient-cured fly ash/blast furnace slag geopolymer pastes can be predicted with relative confidence.

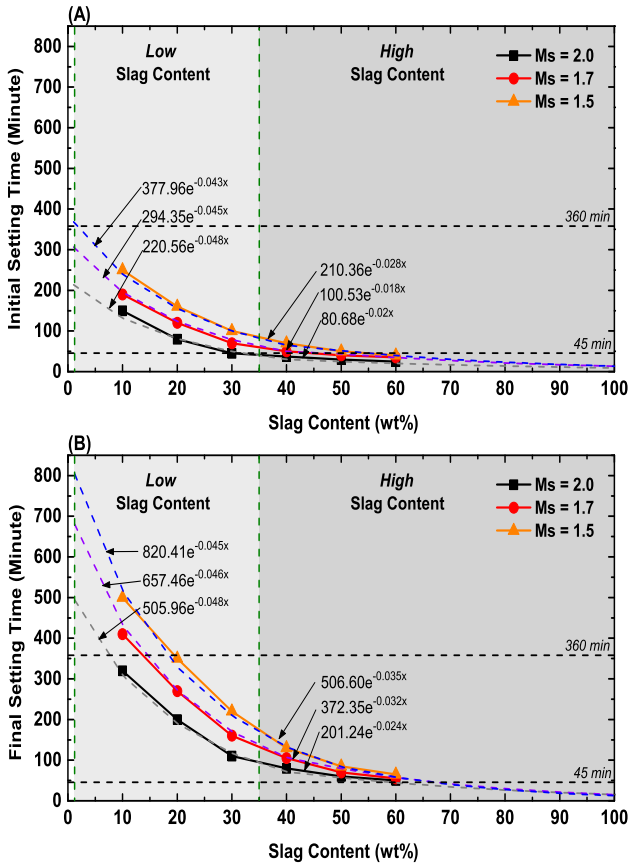

Figure 4. Experimental (solid lines) and calculated (dashed lines) data for (**A**) initial setting time and (**B**) final setting time as a function of blast furnace slag content and Ms (with 30–40 wt% slag as the border between high and low slag contents) for ambient-cured geopolymer pastes. The correlation between experimental and calculated data gives $R^2 > 0.96$. The extrapolations to initial and final setting times at low slag content do not intersect the ordinates, since the chemistry and hence, the model for compositions without slag is different from those with slag.

As will be explained, the observation of two distinct ranges of compressive strength development as a function of blast furnace slag content indicates that there appears to be a mechanistic change in the chemistry of the geopolymerisation process at slag content between 30 and 40 wt% (shown arbitrarily as 35 wt%). Therefore, this is reflected in the application of separate convergent generic equations for the two chemical mechanisms according to the slag content, which is either low or high. The fit between the experimental and calculated data appears to be good as the coefficients of determination are >0.96%.

The Ms values were amalgamated with the data for the generic curves in order to generate master equations for initial and final setting times of ambient-cured geopolymer pastes of low and high slag contents, alkaline activator/SCMs mass ratio of 0.5, and water/binder mass ratio of 0.3; these equations are given in Table 6. These equations can be used to predict the setting times of geopolymer compositions for given blast furnace slag content and Ms. Figure 5 shows the data generated by the use of these master equations for the commonly used Ms of 1.2.

Table 6. Master equations for the prediction of initial and final setting times for ambient-cured geopolymer pastes with low and high slag contents (alkaline activator/supplementary cementitious materials (SCMs) mass ratio of 0.5 and water/binder mass ratio of 0.3).

Setting Time (min)	Low Slag Content (<40 wt% Slag)	High Slag Content (≥40 wt% Slag)
Initial	$(-309.37Ms + 833.9) \times e^{(Slag \times [-0.0100Ms - 0.0280])}$	$(-244.12Ms + 553.7) \times e^{(Slag \times [+0.0142Ms - 0.0466])}$
Final	$(-619.12Ms + 1734.4) \times e^{(Slag \times [-0.0061Ms - 0.0358])}$	$(-607.53Ms + 1413.1) \times e^{(Slag \times [+0.0224Ms - 0.0691])}$

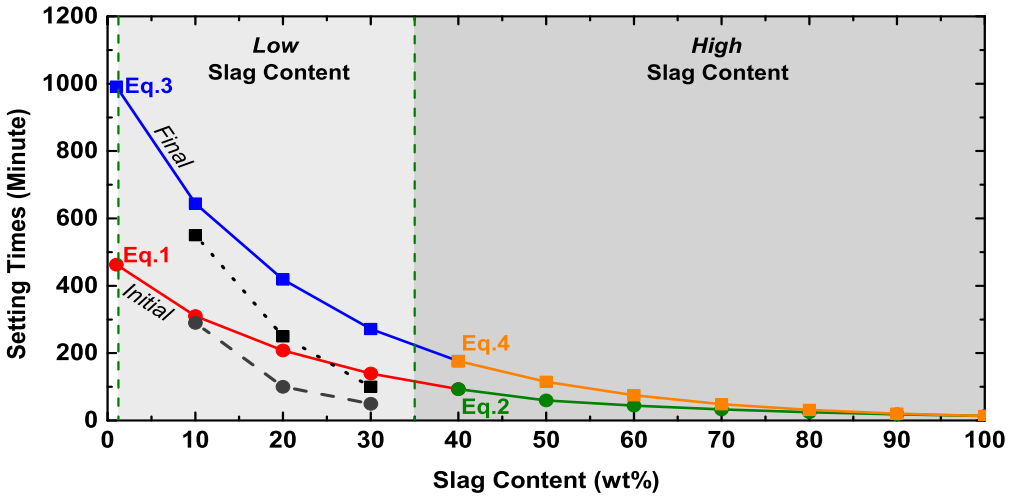

Figure 5. Master plots showing the effect of blast furnace slag content on the setting times of ambient-cured geopolymer pastes of Ms = 1.2, alkaline activator/SCMs mass ratio = 0.5, and water/binder mass ratio = 0.3. Additional experimental data by Nath et al. [40] for initial (dotted lines) and final (dashed lines) setting times at Ms = 1.2, alkaline activator/SCM mass ratio = 0.4, and water/binder mass ratio = 0.2.

The literature relating to the setting time of geopolymer is limited; as a result, the only similar data available for comparison are those of Nath et al. [40]; while the Ms are the same, the alkaline activator/SCMs mass ratio (0.4 vs. 0.5) and the water/binder mass ratio (0.2 vs. 0.3) differ from those of the present work. It is clear that decreasing the two latter parameters decreases both the initial and final setting times. The main differences between these two sets of data are that the data of Nath et al. [40] show shorter setting times, more rapid convergence of the setting times with increasing slag content, and less difference between initial and final setting times. All three of these differences allow the conclusion that increasing the alkaline activator/SCM mass ratio and/or the water/binder mass ratio allows greater flexibility in the mix design.

3.2. Compressive Strength Data

Figure 6A–C (data normalised for sample size) show the compressive strengths of ambient-cured geopolymer mortars as a function of Ms, fly ash/blast furnace slag (FA/S) mass ratio, and age. The rates of compressive strength development were calculated from the first-order derivative of the compressive strength data at the different time points. Taking AS3972 as the more rigorous requirement (Table 2),

it can be seen that all mix designs with ≤20 wt% blast furnace slag were unsuitable, since the compressive strength at 7 days was below 35 MPa. More interestingly, Figure 6A–C show that, at 28 days, five of the six samples with Ms = 1.7 and 1.5 exceed the recommendation, while all of those with Ms = 2.0 fail. This observation indicates that the Ms may be a predictor of compressive strength, which would be expected, but that the data are too limited for further speculation.

Figure 6 also reveals the relative importance of the FA/S mass ratio and the Ms. That is, the data indicate the following:

- Figure 6A–C show that the compressive strengths fall into regimes of low FA/S ratios (high-compressive strengths) and high FA/S ratios (low-compressive strengths).
- Figure 6A–F show that the kinetics of compressive strength development fall into regimes of rapid reaction (1–7 days) and slower reaction (14–28 days).
- Figure 6G–I show that the Ms has a decreasing effect on the rate of compressive strength development as the age increases.
- Figure 6G shows that the FA/S ratio and Ms exhibit competing effects at early age (1–7 days), where:

  High FA/S ratios: Low Ms decreases the rate of compressive strength development.
  Low FA/S ratios: Low Ms increases the rate of compressive strength development.

- Figure 6G also shows that for high FA/S ratios, the early age rate of compressive strength development is greatest for Ms = 1.7.
- Figure 6E suggests that there is a difference between the middle age compressive strength development between the lowest Ms and the two higher Ms. The elucidation of the specific reaction mechanisms of the geopolymerisation process currently is underway. Concerning the present data, it is likely that the geopolymerisation mechanisms can be differentiated between Ms of 1.5 and that of Ms of 1.7 and 2.0. The rapid increase in the rate of strength development between 30 and 40 wt% slag content for Ms of 1.7 and 2.0 suggests that the greater homogeneity of blast furnace slag relative to fly ash and the stress concentrations associated with the presence of crystalline quartz and mullite in the latter [10,66] equate to a shift from an inhomogeneous to a homogeneous microstructure at the transition. Conversely, the absence of the rapid increase in the rate of strength development for Ms of 1.5 results from greater influence of the Ms over that of the mineralogy. This is discussed in more detail below.
- More generally, these data suggest that a minimal slag content of 40 wt% can be expected to yield the most reproducible behaviour and hence, the greatest similarity in geopolymerisation mechanisms.
- Figure 6A–C,G–I demonstrate the highest compressive strengths and the most rapid compressive strength development results from minimal slag contents of 40 wt%.

Examination of Figure 3 shows that slag contents ≥50 wt% are likely to set too quickly to comply with both ASTM C150 and AS 3972. Further, Figure 6A,B show that a slag content of 40 wt% gives a maximal compressive strength at all-time points. Finally, Figure 6A–I indicate that the Ms plays the minor role, which is emphasised by the data in Figure 6A–C. Therefore, the mixes can be divided into two categories according to the dominant roles of the processing variables:

High slag contents: The FA/S ratio plays the dominant role in the compressive strength achieved at all-time points and the Ms plays only a minor role in the rate of strength development. When the setting time and early strength development are considered, the optimal processing conditions are 40 wt% slag and Ms = 1.7.

Low slag contents: Both the FA/S ratio and Ms play significant roles in the compressive strength achieved at all-time points. Examination of the two sets of data spread at constant time points (14–28 days) reveals that at the two higher Ms, the FA/S ratio plays the dominant role, while at the lowest Ms, this variable dominates over the FA/S ratio. When the setting time and the early strength development are considered, the optimal processing conditions are 20–30 wt% slag and Ms = 1.5.

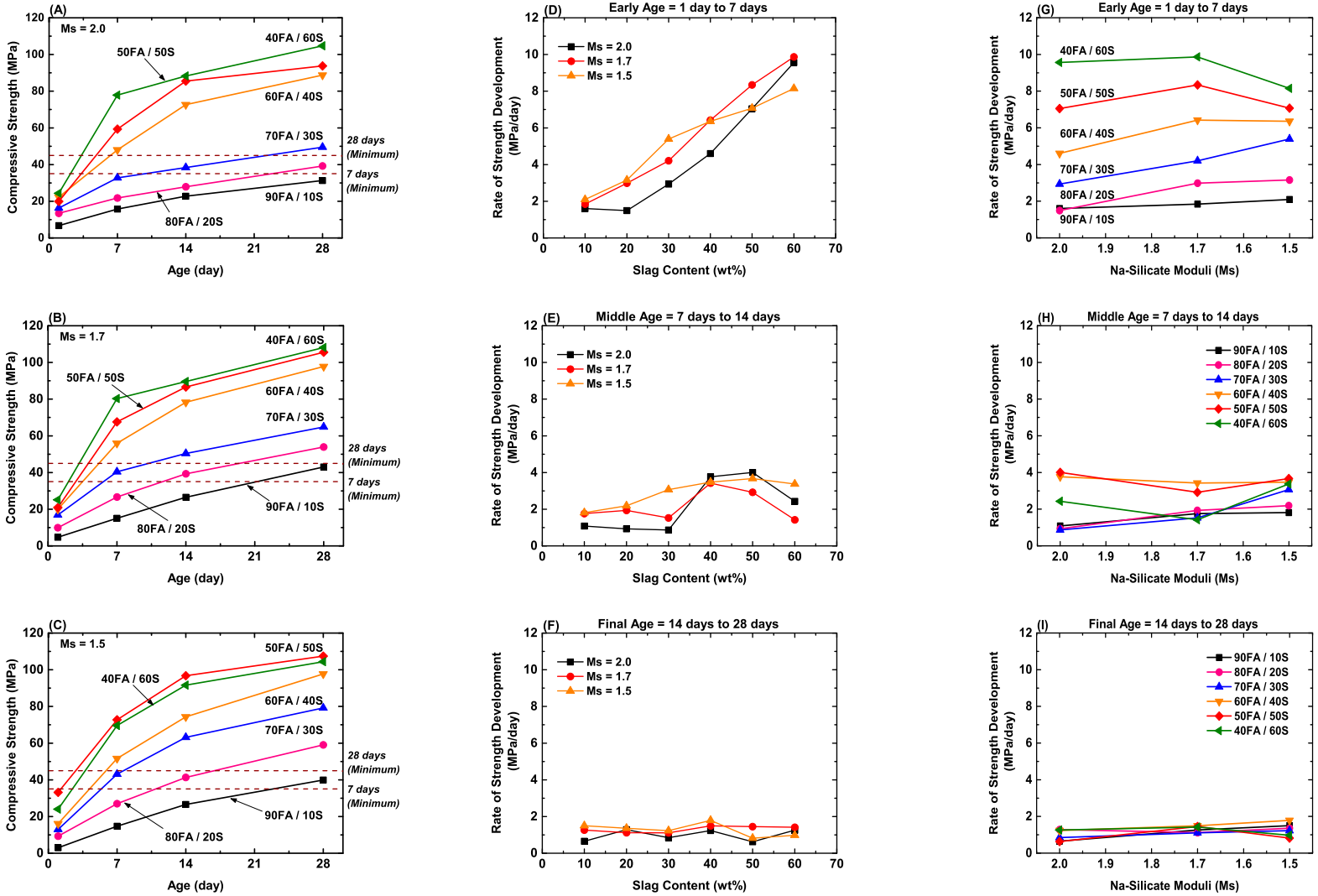

Figure 6. Effects of ageing time on compressive strength (left column, **A**–**C**) and effects of blast furnace slag content (middle column, **D**–**F**) and Ms (right column, **G**–**I**) on the rates of compressive strength development of airtight ambient-cured geopolymer mortars.

Consequently, in terms of mix reproducibility and compressive strength, ambient-cured geopolymer mortars with high blast furnace slag contents (~40 wt%) can be expected to be superior to those with low blast furnace slag contents (~20–30 wt%), since the former mixes will be stronger and subject to the influence of a single variable, while the latter mixes will be weaker and subject to the influences of two dependent experimental variables.

In addition to the compressive strength and setting time considerations, the advantage of high-slag compositions is supported by the mineralogy of blast furnace slag. As mentioned, since blast furnace slag is comparatively more homogeneous than fly ash, then higher slag contents equate to more homogeneous mixes. Additionally, since fly ash contains crystalline quartz and mullite (Figure 1), these residual undissolved species can act as stress concentrators [10,67], again supporting the view that high blast furnace slag contents are advantageous.

Figure 7 compares the effect of blast furnace slag content on the 28-day compressive strengths of geopolymer mortars in the present work and those of other researchers [40,52,54]. It should be noted that in work done by others, the alkaline activator used was sodium silicate solution with Ms in the range 0.96–1.40, which is lower than that used in the present work (1.5–2.0). The variations in the compressive strength with blast furnace slag content appear to approximate a normal distribution, demonstrating that there is a point of diminishing returns for blast furnace slag addition. Excess amounts of blast furnace slag have been shown to have negative impacts not only on the setting time [39,40] but also the compressive strengths [52,53] of ambient-cured geopolymer mortars. Further, it can be seen that the compressive strength increases approximately linearly up to 40 wt% slag, reaching a maximum at 50–60 wt% slag. Although Figures 4 and 5 show an arbitrary border between low and high slag contents at 35 wt%, which indicates a change in chemical mechanism based on the setting time data, it can be assumed that the mechanical properties also would reflect this change in mechanism. Hence, these data suggest that the mechanistic change in chemistry as a function of blast furnace slag content is likely to be closer to 40 wt% rather than 30 wt%.

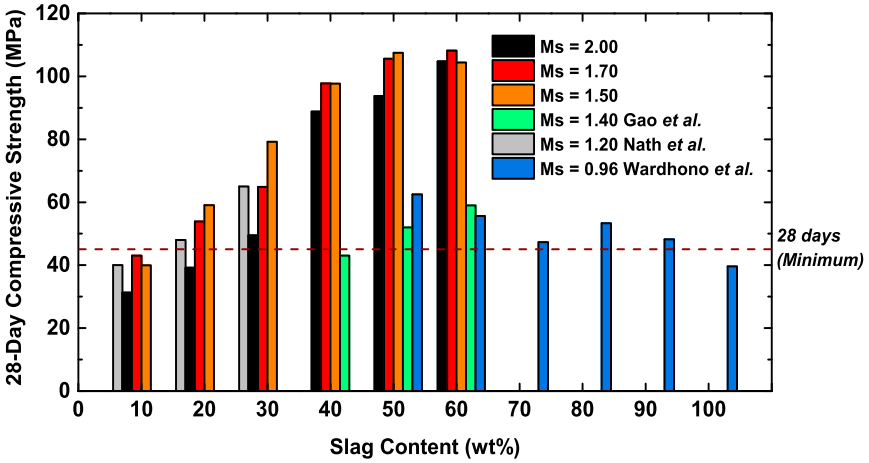

Figure 7. Comparison of effects of blast furnace slag content on 28-day compressive strengths of ambient-cured geopolymer mortars: Present work is compared with data at lower Ms ratios of Ms = 1.20 from Nath et al. [40], Ms = 1.40 from Gao et al. [54], and Ms = 0.96 from Wardhono et al. [52].

The data in Figure 7 also show that the minimal blast furnace slag content to fabricate a geopolymer mortar to meet the compressive strength recommendation stated in AS 3972 is 20 wt% slag for Ms = 1.20–1.70. Geopolymer mortars fabricated using the higher Ms = 2.00 require higher slag contents since these mixes contain insufficient sodium to leach the glass from fly ash. More broadly, these data suggest that the slag content is more important to the compressive strength than the Ms, provided the Ms is ≥1.50. Lower Ms values degrade the compressive strength in general, although the effect is greater at higher blast furnace slag contents. The data reported by Gao et al. [54], which are for

Ms = 1.40, are anomalously low. This probably is a result of the high sand content used, as shown in Table 1.

3.3. Prediction of Long-Term Compressive Strength

Figure 6F,I show that the rates of compressive strength development as a function of blast furnace slag content and Ms converge to similar low rates at 28 days, which suggests that further compressive strength development would be minimal and, according to exponential extrapolation, nearly linear. Consequently, the ultimate compressive strength and curing time, as a function of slag content, is obtained through mathematical derivations, as shown in Online Resource 1. These data are examined in more detail in Figure 8A–D, which show the effects of blast furnace slag content and Ms on the ultimate curing times and compressive strengths. The data in Figure 8A,C support the conclusion that there is a change of mechanism at 30 wt% slag; they also suggest that the Ms is likely to play a key role in the mechanism as both sets of data show that the samples with Ms = 2.0 are different from those of the other two Ms.

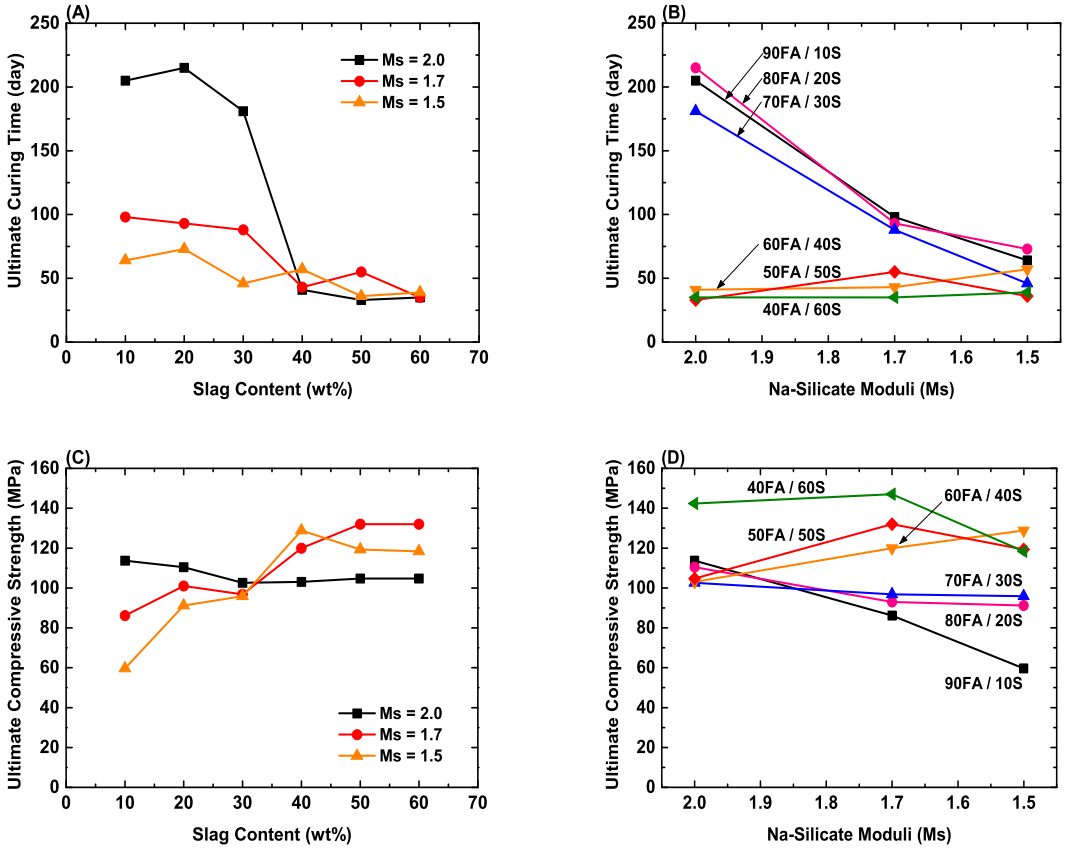

Figure 8. Estimated times for complete curing as a function of: (**A**) blast furnace slag content and (**B**) Ms and estimated ultimate compressive strengths as a function of (**C**) blast furnace slag content and (**D**) Ms of ambient-cured geopolymer mortars based on linear extrapolations (alkaline activator/SCMs mass ratio of 0.5, and water/binder mass ratio of 0.3).

The data in Figure 8B,D emphasise the mechanistic difference between low slag and high slag contents. Figure 8B shows that the effect of Ms for high slag contents is minimal, while for low slag contents, it is notable for the two higher Ms. However, at Ms = 1.5, there is no effect of the slag content. Figure 8C suggests that from Figure 6A–C, for the two higher Ms, it has a relatively small effect on the ultimate compressive strength of high slag contents but that it is more significant for low slag contents. However, for Ms = 1.5, the differentiation between the low and high slag contents is reduced.

Figure 8A emphasises that in terms of the curing time, there appears to be little advantage in increasing the slag content beyond 40 wt% blast furnace slag. In contrast, Figure 8C suggests that while the slag content has little effect on the ultimate compressive strength for Ms = 1.5, further strength increases could be expected with increased slag contents for the two higher Ms.

Figure 8C indicates that Ms values lower than 1.5 can be expected to show little effect from the slag content and therefore, the ultimate curing times would be minimised and consistent. Figure 8D suggests that both Ms and blast furnace slag content are important to the ultimate compressive strength. That is, while decreasing the Ms generally decreases the strength at all blast furnace slag contents, this deleterious effect is mitigated at intermediate blast furnace slag contents (20–40 wt%).

Contrasting the data in Figure 4, Figure 5, Figure 6D–F and Figure 8A,C, it can be seen that the influences of the FA/S ratio and Ms on the setting time (Figures 4 and 5), rate of strength development (Figure 6D–F), ultimate curing time (viz., age) (Figure 8A), and ultimate compressive strength (Figure 8C) reveal behaviour and inflections that are similar but not identical. This is likely to be a result of the competing effects of FA/S ratio and Ms, which dominate differently according to the experimental parameters.

4. Conclusions

4.1. Mix Design

The present work demonstrates that ambient-cured geopolymer mortars can be fabricated without the need for high alkalinity activators (Ms = 0.96–1.40) or thermal curing, provided that the FA/S mass ratio and Ms are appropriately balanced. Figure 9 summarises the feasibility of mix designs used in present work. These are classified into five different regions:

1. These mixes fail to meet both the final setting time and compressive strength requirements due to sluggish kinetics.
2. These mixes have the most flexible setting times, but they fail to meet the compressive strength requirement.
3. These mixes have high compressive strengths but, owing to the high blast furnace slag content, they set too quickly; also, there is no strength increase at slag contents >50 wt%.
4. These mixes exhibit the most flexible setting times for those that meet the compressive strength requirement; however, at the slag content of 30 wt%, the compressive strengths depend on the Ms (Figure 6), which makes the process sensitive to the alkalinity of the activator.
5. These mixes pass both the setting time and strength requirements, representing reproducible mix designs in terms of both blast furnace slag content and Ms; the mix in region 6 is optimal in that it shows the highest extrapolated ultimate compressive strength (~132 MPa at 60FA/40S at Ms = 1.7).

4.2. Predictive Models

Predictive models for initial and final setting times and for compressive strengths of ambient-cured geopolymer pastes and mortars have been developed. They are based on curve-fitting and extrapolations of the experimental data for these parameters in terms of the fly ash/slag mass ratio and Ms. The extrapolations of these data, illustrated by Figure 4, Figure 5, Figure 8 and Supplementary Figure S1, emphasise that modulation of the FA/S ratio with the Ms can yield practical setting times, adequate rates of compressive strength development, and adequate ultimate compressive strengths. These predictive models provide the platform for the assessment of these data for materials scientists, civil engineers, and others who are investigating geopolymer cements and concretes. Since these models are new to the literature, directions for further work include:

- Variation of the alkaline activator/SCMs mass ratio;
- Variation of the water/binder mass ratio;

- Interpolative refinement of the Ms <1.50 and in the range 1.70–2.00;
- Variation of combined Ms and blast furnace slag content in order to determine effects on drying shrinkage [7], efflorescence [59], and long-term durability [72];
- Optimisation of the sand/SCMs mass ratio <2.00 [63];
- Alteration of the alkaline activator from sodium silicate to potassium silicate;
- Variation in the fly ash type (Class C, Class F), mineralogy, glass chemistry, and particle size/surface area;
- Variation of the slag mineralogy, glass chemistry, and particle size/surface area.

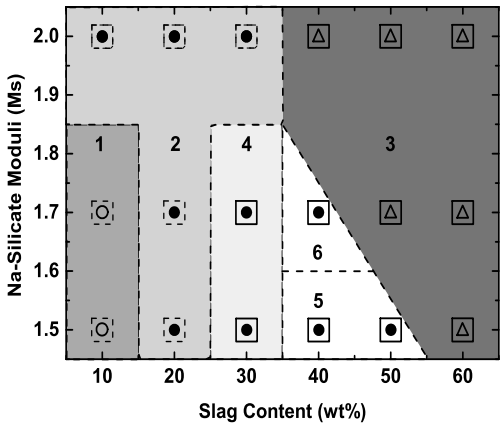

Figure 9. Summary of initial (triangles) and final setting (circles) times and compressive strengths (boxes) of ambient-cured geopolymer pastes and mortars according to pass/fail of criteria of AS 3972 (alkaline activator/SCMs mass ratio of 0.5, and water/binder mass ratio of 0.3). Criterion: (**pass**) initial/final setting time ●; compressive strength □; (**fail**) initial setting time △; final setting time ○; compressive strength ⬚.

The preceding comments highlight the critical role played by the balance between the FA/S mass ratio and the Ms, as shown by the experimental variables examined, being the initial and final setting times, compressive strength development, and ultimate compressive strengths. The present work reveals that it is possible to generalise the roles of FA/S mass ratio and the Ms to predict the resultant development of the characteristics of geopolymers.

Supplementary Materials: The following are available online at http://www.mdpi.com/2075-163X/10/10/920/s1, Figure S1: Rate of compressive strength development (bold lines) and extrapolated values (dashed lines) as a function of age and Ms (alkaline activator/SCMs mass ratio of 0.5, and water/binder mass ratio of 0.3) of ambient-cured geopolymer mortars, Table S1: Percentage error between experimental and interpolated data.

Author Contributions: S.U. undertook the experimentation, prepared the first draft, and contributed to subsequent drafts. P.K. co-supervised the project and contributed to all subsequent drafts. A.R. supervised the supporting NMR aspects of the project. A.C. contributed to all subsequent drafts. C.C.S. supervised the project, prepared the first draft, and contributed to subsequent drafts. All authors have read and agreed to the published version of the manuscript.

Funding: This research work is partially funded by the Cooperative Research Centre (CRC) for Low Carbon Living, an Australian Government initiative (grant number RP1020).

Acknowledgments: The lead author also would like to thank UNSW Sydney for the University International Postgraduate Award that supported this work. The authors also are grateful for the subsidised facilities for characterisation provided by the Mark Wainwright Analytical Centre, UNSW Sydney.

Conflicts of Interest: The authors declare no conflict of interest.

References

1. McLellan, B.C.; Williams, R.P.; Lay, J.; van Riessen, A.; Corder, G.D. Costs and Carbon Emissions for Geopolymer Pastes in Comparison to Ordinary Portland Cement. *J. Clean. Prod.* **2011**, *19*, 1080–1090. [CrossRef]
2. Müller, N.; Harnisch, J. *A Blueprint for a Climate Friendly Cement Industry*; WWF International: Gland, Switzerland, 2007.
3. Thomas, M. *Supplementary Cementing Materials in Concrete*; CRC Press: Boca Raton, FL, USA, 2013.
4. Aldred, J.; Day, J. Is Geopolymer Concrete a Suitable Alternative to Traditional Concrete? In Proceedings of the 37th Conference on Our World in Concrete & Structures, Singapore, 29–31 August 2012; pp. 29–31.
5. Milliken Infrastructure Solutions. *Milliken GeoSprayTM Geopoymer Mortar: GeoSpray™ Geopolymer Mortar System for Structural Rehabilitation of Sewer and Storm Water Infrastructure*; Milliken Infrastructure Solutions: Lafayette, CO, USA, 2013.
6. Kosmatka, S.H.; Kerkhoff, B.; Panarese, W.C. *Design and Control of Concrete Mixtures*, 14th ed.; Portland Cement Association: Skokie, IL, USA, 2008.
7. Davidovits, J. *Geopolymer Chemistry and Applications*, 2nd ed.; Institut Geopolymere: Saint-Quentin, France, 2008.
8. Pavel, R. Effect of Curing Temperature on the Development of Hard Structure of Metakolin-Based Geopolymer. *Constr. Build. Mater.* **2010**, *24*, 1176–1183.
9. Bakria, A.M.M.A.; Kamarudin, H.; BinHussain, M.; Nizar, I.K.; Zarina, Y.; Rafiza, A.R. The Effect of Curing Temperature on Physical and Chemical Properties of Geopolymers. *Phys. Procedia* **2011**, *22*, 286–291. [CrossRef]
10. Ismail, I.; Bernal, S.A.; Provis, J.L.; San Nicolas, R.; Hamdan, S.; van Deventer, J.S.J. Modification of Phase Evolution in Alkali-Activated Blast Furnace Slag by the Incorporation of Fly Ash. *Cem. Concr. Compos.* **2014**, *45*, 125–135. [CrossRef]
11. Temuujin, J.; van Riessen, A. Effect of Fly Ash Preliminary Calcination on the Properties of Geopolymer. *J. Hazard. Mater.* **2009**, *164*, 634–639. [CrossRef]
12. Görhan, G.; Kürklü, G. The Influence of the NaOH Solution on the Properties of the Fly Ash-Based Geopolymer Mortar Cured at Different Temperatures. *Compos. B. Eng.* **2014**, *58*, 371–377. [CrossRef]
13. Temuujin, J.; Williams, R.P.; van Riessen, A. Effect of Mechanical Activation of Fly Ash on the Properties of Geopolymer Cured at Ambient Temperature. *J. Mater. Process. Technol.* **2009**, *209*, 5276–5280. [CrossRef]
14. Temuujin, J.; van Riessen, A.; Williams, R. Influence of Calcium Compounds on the Mechanical Properties of Fly Ash Geopolymer Pastes. *J. Hazard. Mater.* **2009**, *167*, 82–88. [CrossRef]
15. Kingery, W.D. *Introduction to Ceramics*; Wiley: New York, NY, USA, 1960.
16. Duxson, P.; Provis, J.L.; Lukey, G.C.; van Deventer, J.S.J. The Role of Inorganic Polymer Technology in the Development of 'Green Concrete'. *Cem. Concr. Res.* **2007**, *37*, 1590–1597. [CrossRef]
17. Turner, L.K.; Collins, F.G. Carbon Dioxide Equivalent (CO_2-e) Emissions: A Comparison between Geopolymer and OPC Cement Concrete. *Constr. Build. Mater.* **2013**, *43*, 125–130. [CrossRef]
18. Provis, J.L.; Palomo, A.; Shi, C. Advances in Understanding Alkali-Activated Materials. *Cem. Concr. Res.* **2015**, *78*, 110–125. [CrossRef]
19. Ouellet-Plamondon, C.; Habert, G. Chapter 25—Life Cycle Assessment (LCA) of Alkali-Activated Cements and Concretes. In *Handbook of Alkali-Activated Cements, Mortars and Concretes*; Pacheco-Torgal, F., Labrincha, J., Leonelli, C., Palomo, A., Chindaprasit, P., Eds.; Woodhead Publishing: Oxford, UK, 2015; pp. 663–686.
20. Gartner, E. Industrially Interesting Approaches to "Low-CO_2" Cements. *Cem. Concr. Res.* **2004**, *34*, 1489–1498. [CrossRef]
21. Lyon, R.E.; Balaguru, P.N.; Foden, A.; Sorathia, U.; Davidovits, J.; Davidovics, M. Fire-Resistant Aluminosilicate Composites. *Fire Mater.* **1997**, *21*, 67–73. [CrossRef]
22. Chindaprasirt, P.; Chareerat, T.; Hatanaka, S.; Cao, T. High-Strength Geopolymer Using Fine High-Calcium Fly Ash. *J. Mater. Civ. Eng.* **2011**, *23*, 264–270. [CrossRef]
23. Davidovits, J.; Davidovits, R.; Davidovits, M. Geopolymeric Cement Based on Fly Ash and Harmless to Use. U.S. Patent 8,202,362 B2, 19 June 2012.
24. Heidrich, C.; Feuerborn, H.-J.; Weir, A. Coal Combustion Products: A Global Perspective. In Proceedings of the 2013 World Coal Ash (WOCA) Conference, Lexington, KY, USA, 22–25 April 2013; pp. 22–25.

25. Diaz, E.I.; Allouche, E.N.; Eklund, S. Factors Affecting the Suitability of Fly Ash as Source Material for Geopolymers. *Fuel* **2010**, *89*, 992–996. [CrossRef]
26. Duxson, P.; Provis, J.L. Designing Precursors for Geopolymer Cements. *J. Am. Ceram. Soc.* **2008**, *91*, 3864–3869. [CrossRef]
27. Kong, D.L.Y.; Sanjayan, J.G. Effect of Elevated Temperatures on Geopolymer Paste, Mortar and Concrete. *Cem. Concr. Res* **2010**, *40*, 334–339. [CrossRef]
28. Bakharev, T. Thermal Behaviour of Geopolymers Prepared using Class F Fly Ash and Elevated Temperature Curing. *Cem. Concr. Res.* **2006**, *36*, 1134–1147.
29. Somna, K.; Jaturapitakkul, C.; Kajitvichyanukul, P.; Chindaprasirt, P. NaOH-Activated Ground Fly Ash Geopolymer Cured at Ambient Temperature. *Fuel* **2011**, *90*, 2118–2124.
30. Xie, J.; Kayali, O. Effect of Initial Water Content and Curing Moisture Conditions on the Development of Fly Ash-Based Geopolymers in Heat and Ambient Temperature. *Constr. Build. Mater.* **2014**, *67*, 20–28. [CrossRef]
31. Puertas, F.; Martínez-Ramírez, S.; Alonso, S.; Vázquez, T. Alkali-Activated Fly Ash/Slag Cements: Strength Behaviour and Hydration Products. *Cem. Concr. Res* **2000**, *30*, 1625–1632. [CrossRef]
32. Noushini, A.; Babaee, M.; Castel, A. Suitability of Heat-Cured Low-Calcium Fly Ash-Based Geopolymer Concrete for Precast Applications. *Mag. Concr. Res.* **2016**, *68*, 163–177. [CrossRef]
33. Wallah, S.; Rangan, B.V. *Low-Calcium Fly Ash-Based Geopolymer Concrete: Long-Term Properties*; Curtin University of Technology: Perth, Australia, 2006.
34. Fernández-Jiménez, A.; Garcia-Lodeiro, I.; Palomo, A. Durability of Alkali-Activated Fly Ash Cementitious Materials. *J. Mater. Sci.* **2007**, *42*, 3055–3065. [CrossRef]
35. Sumajouw, D.M.J.; Hardjito, D.; Wallah, S.E.; Rangan, B.V. Fly Ash-Based Geopolymer Concrete: Study of Slender Reinforced Columns. *J. Mater. Sci.* **2007**, *42*, 3124–3130.
36. Castel, A.; Foster, S.J.; Ng, T.; Sanjayan, J.G.; Gilbert, R.I. Creep and Drying Shrinkage of a Blended Slag and Low Calcium Fly Ash Geopolymer Concrete. *Mater. Struct.* **2016**, *49*, 1619–1628. [CrossRef]
37. Sarker, P.K.; Haque, R.; Ramgolam, K.V. Fracture Behaviour of Heat Cured Fly Ash Based Geopolymer Concrete. *Mater. Des.* **2013**, *44*, 580–586. [CrossRef]
38. Castel, A.; Foster, S.J. Bond Strength between Blended Slag and Class F Fly Ash Geopolymer Concrete with Steel Reinforcement. *Cem. Concr. Res.* **2015**, *72*, 48–53. [CrossRef]
39. Kumar, S.; Kumar, R.; Mehrotra, S. Influence of Granulated Blast Furnace Slag on the Reaction, Structure and Properties of Fly Ash Based Geopolymer. *J. Mater. Sci.* **2010**, *45*, 607–615. [CrossRef]
40. Nath, P.; Sarker, P.K. Effect of GGBFS on Setting, Workability and Early Strength Properties of Fly Ash Geopolymer Concrete Cured in Ambient Condition. *Constr. Build. Mater.* **2014**, *66*, 163–171. [CrossRef]
41. Fernández-Jiménez, A.; Puertas, F.; Sobrados, I.; Sanz, J. Structure of Calcium Silicate Hydrates Formed in Alkaline-Activated Slag: Influence of the Type of Alkaline Activator. *J. Am. Ceram. Soc.* **2003**, *86*, 1389–1394. [CrossRef]
42. Liebau, F. *Structural Chemistry of Silicates: Structure, Bonding, and Classification*; Springer: Berlin/Heidelberg, Germany, 1985.
43. De Silva, P.; Sagoe-Crenstil, K.; Sirivivatnanon, V. Kinetics of Geopolymerization: Role of Al_2O_3 and SiO_2. *Cem. Concr. Res.* **2007**, *37*, 512–518. [CrossRef]
44. Gao, X.; Yu, Q.; Brouwers, H. Reaction Kinetics, Gel Character and Strength of Ambient Temperature Cured Alkali Activated Slag–Fly Ash Blends. *Constr. Build. Mater.* **2015**, *80*, 105–115. [CrossRef]
45. Phoo-ngernkham, T.; Sata, V.; Hanjitsuwan, S.; Ridtirud, C.; Hatanaka, S.; Chindaprasirt, P. High Calcium Fly Ash Geopolymer Mortar Containing Portland Cement for Use as Repair Material. *Constr. Build. Mater.* **2015**, *98*, 482–488. [CrossRef]
46. Giasuddin, H.M.; Sanjayan, J.G.; Ranjith, P.G. Strength of Geopolymer Cured in Saline Water in Ambient Conditions. *Fuel* **2013**, *107*, 34–39. [CrossRef]
47. Kumar, R.; Kumar, S.; Mehrotra, S.P. Towards Sustainable Solutions for Fly Ash through Mechanical Activation. *Resour. Conserv. Recycl.* **2007**, *52*, 157–179. [CrossRef]
48. Yip, C.K.; Lukey, G.C.; Provis, J.L.; van Deventer, J.S.J. Effect of Calcium Silicate Sources on Geopolymerisation. *Cem. Concr. Res.* **2008**, *38*, 554–564. [CrossRef]
49. Suwan, T.; Fan, M. Influence of OPC Replacement and Manufacturing Procedures on the Properties of Self-Cured Geopolymer. *Constr. Build. Mater.* **2014**, *73*, 551–561. [CrossRef]

50. Inti, S.; Sharma, M.; Tandon, V. Influence of Curing on the Properties of Geopolymer Mortar Made with Low Molarity Sodium Hydroxide. *Transp. Dev. Econ.* **2017**, *3*, 11. [CrossRef]
51. Morsy, M.S.; Alsayed, S.H.; Al-Salloum, Y.; Almusallam, T. Effect of Sodium Silicate to Sodium Hydroxide Ratios on Strength and Microstructure of Fly Ash Geopolymer Binder. *Arab. J. Sci. Eng.* **2014**, *39*, 4333–4339. [CrossRef]
52. Wardhono, A.; Law, D.W.; Strano, A. The Strength of Alkali-activated Slag/fly Ash Mortar Blends at Ambient Temperature. *Procedia Eng.* **2015**, *125*, 650–656. [CrossRef]
53. Chi, M.C.; Liu, Y.C. Effects of Fly Ash/Slag Ratio and Liquid/Binder Ratio on Strength of Alkali-Activated Fly Ash/Slag Mortars. *Appl. Mech. Mater.* **2013**, *377*, 50–54. [CrossRef]
54. Gao, X.; Yu, Q.L.; Brouwers, H.J.H. Properties of Alkali Activated Slag–Fly Ash Blends with Limestone Addition. *Cem. Concr. Compos.* **2015**, *59*, 119–128. [CrossRef]
55. ASTM C150/C150M-12. *Standard Specification for Portland Cement*; ASTM International: West Conshohocken, PA, USA, 2012.
56. AS 3972-2010. *General Purpose and Blended Cements*; Standards Australia Limited: Sydney, Australia, 2010.
57. Diamond, S. On the Glass Present in Low-Calcium and in High-Calcium Flyashes. *Cem. Concr. Res.* **1983**, *13*, 459–464. [CrossRef]
58. ASTM C128-15. *Standard Test Method for Relative Density (Specific Gravity) and Absorption of Fine Aggregate*; ASTM International: West Conshohocken, PA, USA, 2015.
59. Zhang, Z.; Provis, J.L.; Reid, A.; Wang, H. Geopolymer Foam Concrete: An Emerging Material for Sustainable Construction. *Constr. Build. Mater.* **2014**, *56*, 113–127. [CrossRef]
60. Provis, J.L.; Yong, C.Z.; Duxson, P.; van Deventer, J.S.J. Correlating Mechanical and Thermal Properties of Sodium Silicate-Fly Ash Geopolymers. *Colloids Surf. A* **2009**, *336*, 57–63. [CrossRef]
61. Xie, Z.; Xi, Y. Hardening Mechanisms of an Alkaline-Activated Class F Fly Ash. *Cem. Concr. Res.* **2001**, *31*, 1245–1249. [CrossRef]
62. Sun, P. Fly Ash Based Inorganic Polymeric Building Material. Ph.D. Thesis, Wayne State University, Detroit, MI, USA, 2005.
63. Thakur, R.N.; Ghosh, S. Effect of Mix Composition on Compressive Strength and Microstructure of Fly Ash Based Geopolymer Composites. *Int. J. Appl. Eng. Res.* **2009**, *4*, 68–74.
64. Temuujin, J.; van Riessen, A.; MacKenzie, K.J.D. Preparation and Characterisation of Fly Ash Based Geopolymer Mortars. *Constr. Build. Mater.* **2010**, *24*, 1906–1910. [CrossRef]
65. ASTM C191-13. *Standard Test Methods for Time of Setting of Hydraulic Cement by Vicat Needle*; ASTM International: West Conshohocken, PA, USA, 2013.
66. ASTM C109/C109M-13. *Standard Test Method for Compressive Strength of Hydraulic Cement Mortars (Using 2-in. or [50-mm] Cube Specimens)*; ASTM International: West Conshohocken, PA, USA, 2013.
67. Morrell, R. *Handbook of Properties of Technical and Engineering Ceramics*; H.M. Stationary Office: Ann Arbor, MI, USA, 1985.
68. Hamad, A.J. Size and Shape Effect of Specimen on the Compressive Strength of HPLWFC Reinforced with Glass Fibres. *J. King Saud Univ. Eng. Sci.* **2017**, *29*, 373–380. [CrossRef]
69. Fernández-Jiménez, A.M.; Palomo, A.; López-Hombrados, C. Engineering Properties of Alkali-Activated Fly Ash Concrete. *ACI Mater.* **2006**, *103*, 106–112.
70. Rao, G.M.; Rao, T.D.G. Final Setting Time and Compressive Strength of Fly Ash and GGBS-Based Geopolymer Paste and Mortar. *Arab. J. Sci. Eng.* **2015**, *40*, 3067–3074.
71. Criado, M.; Fernández-Jiménez, A.; Palomo, A. Alkali Activation of Fly Ash: Effect of the SiO_2/Na_2O Ratio: Part I: FTIR Study. *Micropor. Mesopor. Mater.* **2007**, *106*, 180–191. [CrossRef]
72. Dong, M.; Elchalakani, M.; Karrech, A. Development of High Strength One-Part Geopolymer Mortar using Sodium Metasilicate. *Constr. Build. Mater.* **2020**, *236*, 117611. [CrossRef]